10-1-2007

Simulation of Plasticity in Nanocrystalline Silicon

M. J. Demkowicz
Los Alamos National Laboratory

A. S. Argon
Massachusetts Institute of Technology

D. Farkas
Virginia Polytechnic Institute and State University

Megan Frary
Boise State University

Simulation of Plasticity in Nanocrystalline Silicon

M. J. DEMKOWICZ*[1], A. S. ARGON[2], D. FARKAS[3], M. FRARY[4]

[1]MST-8: Structure-Property Relations Group, Los Alamos National Laboratory, Los Alamos, NM 87545

[2]Department of Mechanical Engineering, Massachusetts Institute of Technology, Cambridge, MA 02139

[3]Department of Materials Science and Engineering, Virginia Polytechnic Institute and State University, Blacksburg, VA 24061

[4]Department of Materials Science and Engineering, Boise State University, Boise, ID 83725

Molecular dynamics investigation of plasticity in a model nanocrystalline silicon system demonstrates that inelastic deformation localizes in intergranular regions. The carriers of plasticity in these regions are atomic environments that can be described as high-density liquid-like amorphous silicon. During fully developed flow, plasticity is confined to system-spanning intergranular zones of easy flow. As an active flow zone rotates out of the plane of maximum resolved shear stress during deformation to large strain, new zones of easy flow are formed. Compatibility of the microstructure is accommodated by processes such as grain rotation and formation of new grains. Nano-scale voids or cracks may form if there emerge stress concentrations that cannot be relaxed by a mechanism that simultaneously preserves microstructural compatibility.

Keywords: Plasticity; Silicon; Molecular dynamics; Nanocrystalline; Grain boundary; Microstructural compatibility

1. Introduction

In polycrystalline materials with characteristic grain sizes larger than a few hundred nanometers—i.e. 'microcrystalline' materials—the initial yield and cleavage stresses as well as the plastic flow stress rise with decreasing characteristic grain size. In initial yield and cleavage, this rise results from the role played by dislocation pileups in creating stress concentrations at grain boundaries [1, 2]. The rise in flow stress, on the other hand, is associated with the increasing difficulty of accommodating compatibility between neighboring deforming crystal grains through the aggregation of geometrically-necessary dislocations [3]. In the microcrystalline regime, the initial yield and cleavage stresses as well as the flow stresses vary with the inverse square root of the grain size, even though the mechanistic justification for this relation differs in both cases.

Recently, extensive research efforts have been devoted to the goal of understanding the mechanical properties of 'nanocrystalline' materials, i.e. polycrystalline materials whose characteristic grain size is within the range of a few nanometers to several tens of nanometers. Of particular interest has been the possibility—confirmed in computer simulations [4]—that at a specific value of characteristic grain size referred to as the 'strongest size' [5] nanocrystalline materials attain their maximum strength, measured in terms of yield stress or flow stress.

In nanocrystalline materials whose grain sizes are below their 'strongest size' value and approach the extreme lower limit of a few nanometers, plastic flow is no longer accomplished through the motion of dislocations. Instead, in such solids flow occurs through the deformation of grain boundary material: a process sometimes referred to as 'grain boundary sliding' [6]. This form of plasticity alone may be able to accommodate plastic flow to 'large' strain (i.e. plastic strain much larger than the initial yield strain) in materials whose grain sizes are so low that the total volume fraction of grain boundary material is on the order of several tens of percent. Unlike dislocation motion, however, grain boundary plasticity by itself is

not capable of ensuring compatibility between neighboring crystal grains in larger-grained materials. Therefore, as the characteristic grain size of a material increases above the lower limit of a few nanometers, microstructural compatibility is accommodated through a variety of processes, such as deformation-induced formation of new crystal grains [7]. Dislocation nucleation and propagation also become increasingly essential—despite considerable energy barriers [8]—if the material is to remain intact during plastic flow. The 'strongest size' phenomenon itself occurs at a characteristic grain size where dislocation-based plasticity and grain boundary sliding take place at equal stresses [9].

The work presented here explores grain boundary plasticity and accommodation of microstructural compatibility during plastic flow in a model nanocrystalline material with grain sizes below its strongest size. In contrast to most previous studies of plasticity in nanocrystalline materials, however, the current work concerns deformation of a model covalently bonded material—namely silicon—rather than a model metal. There are several reasons for this difference in focus. First, since the lattice resistance of covalently bonded materials [10] is higher than in metals, modes of accommodating microstructural compatibility through processes other than dislocation nucleation and motion are likely to be favored. Second, unlike metals, fully-dense covalently-bonded nanocrystalline materials with controlled grain sizes as low as 3nm can be reproducibly created allowing for direct comparison of experimental and modeling results for the range of grain sizes of interest [11]. Finally, understanding of the mechanical behaviour of covalently-bonded nanocrystalline materials is essential in several areas of technological importance, for example in explaining the ultrahardness of nanocomposites used to coat machine tools [12] or in understanding the fatigue and fracture properties of the nanocrystalline Si used in MEMS devices and photovoltaics [13].

2. Modeling and analysis methods

The simulations described here were carried out using the Stillinger-Weber (SW) potential for silicon [14]. This potential was chosen over other available potentials [15-17] due to its simple form, the large accumulated body of knowledge concerning its behaviour, and its ability to reproduce—in broad brushstrokes—the behaviour of silicon across a range of externally applied conditions [18-22]. Furthermore, this potential was successfully applied in a series of studies on plasticity of amorphous silicon (a-Si) that will be useful in interpreting the results presented here [23-26].

Plastic deformation was carried out using molecular dynamics (MD) simulations at a temperature of 300K using time steps of 3.87 fs. Since the equilibrium melting temperature of SW Si is known to be about 1690 K [27], the temperature at which the simulations were carried out corresponds to a homologous temperature of ~0.18 and is well within the range characteristic of low-temperature plasticity [28]. Deformation was applied externally to the simulation cell under periodic boundary conditions by imposing small increments of volume-preserving plane strain [29]. Each deformation increment consisted of an extension in the y-direction of $d\varepsilon_y = 10^{-3}$, a corresponding contraction in the x-direction of $d\varepsilon_x = -d\varepsilon_y \big/ \left(1 + d\varepsilon_y\right)$, and no deformation in the z-direction. After every such deformation increment, the atomic configuration was re-equilibrated by MD subject to the constraint of constant volume and invariant simulation cell shape. By monitoring the evolution of quantities such as total potential energy, system pressure, and deviatoric stress it was determined that 1000 time steps suffice to re-equilibrate the model system after a strain increment was applied. The above process was repeated 700 times, resulting in a total deviatoric strain of 117% for each deformation simulation. The described procedure corresponds to a strain rate of about $2.58 \cdot 10^8$ s^{-1}, which is much greater than that found in most experimentally attainable situations. It is too rapid to probe thermally activated plasticity or viscoelastic relaxations. Since it is carried out at a low homologous temperature, however, it serves as a useful method of investigating plasticity in the athermal limit.

After a particular nc-Si system had been deformed well beyond its initial yield strain (i.e. to 'large strain'), its mechanical behaviour was characterized using a number of system-scale and atomic-level quantities. The overall stress tensor was determined analytically by direct calculation from the interatomic potential [30]. This tensor can be decomposed into atomic-level stress tensors in a way analogous to that used by Maeda and Takeuchi [31] and described in detail elsewhere [24]. The total stress in any region of the simulated material can be found by performing a volume average of the atomic stresses in that region. The volume-average over all atomic-level stresses returns the overall system stress.

Hydrostatic and deviatoric components can be determined for the stress tensor τ by applying the following formulas [29]:

$$p(\tau) = -\tfrac{1}{3} tr(\tau)$$
$$\bar{\sigma}(\tau) = \left| \tau - \tfrac{1}{3} tr(\tau)\mathbf{I} \right|$$

The same formulas can be used to evaluate the hydrostatic and deviatoric components of any other rank-two tensor quantity, such as atomic level stresses or overall system strains. Total system deviatoric strains shall be denoted as $\bar{\varepsilon}(\varepsilon)$.

As will be shown in section 4.1, certain regions of the model nanocrystalline Si (nc-Si) atomic configuration undergoing plastic flow can be described as being amorphous (a-Si). In previous studies [23, 24] it was found that a-Si is composed of two distinct and unambiguously distinguishable atomic environments: 'liquid-like' a-Si and 'solid-like' a-Si. Whether a particular atom is solid-like or liquid-like is determined from the average and standard deviation of its nearest neighbor bond angles using a procedure detailed elsewhere [24]. Although both liquid-like and solid-like environments correspond to a-Si configurations that are vitrified, the structure of the former resembles that of molten silicon while the later resembles diamond cubic crystalline silicon. In particular, liquid-like a-Si is approximately 5-fold coordinated and more dense than solid-like a-Si, in analogy with the fact that molten silicon is denser than diamond cubic crystalline silicon [32]. Meanwhile, solid-like a-Si is on average 4-fold coordinated and less dense than liquid-like a-Si. By determining the liquid-like or solid-like character of each atomic environment in an a-Si configuration, the system-wide mass fraction of liquid-like environments ϕ may be defined. It has been shown that a-Si configurations with high values of ϕ are more amenable to plastic flow than those with lower values of ϕ, indicating that liquid-like atomic environments can be viewed as the carriers of plasticity in a-Si. The mass fraction of liquid-like environments ϕ will be used in analyzing the results obtained in the course of this study.

Plasticity in glassy materials proceeds by localized rearrangements in small atomic clusters [25, 33-37]. To distinguish these clusters from material whose deformation is purely elastic, a method based on the formalism of the Eshelby inclusion problem [38] was applied. In this scheme—described in detail in reference 25—the resultant forces on atoms in two configurations that differ by a slight plastic strain increment are compared. If the difference in these forces Δf for some specific atomic site is well-accounted for (to within some arbitrary, but conservatively chosen tolerance) by the linear elastic prediction

$$\Delta f = -H \cdot d,$$

where H is the system Hessian matrix and d the vector of incremental atomic displacements between the two configurations under consideration, then the neighborhood of that atomic site is said to have deformed elastically and is counted as part of the *elastically deforming matrix material* for the inelastic event in question. A certain number of atomic sites will not satisfy this criterion, though. These sites are counted as comprising the *inelastically transforming inclusion*.

3. Model quasi-columnar nanocrystalline silicon system

Similar to the approach adopted by Yamakov *et al.* for nanocrystalline metals [7], the present study investigates the plastic response of a quasi-columnar model system. A visualization of this model nc-Si structure is shown in figure 1. The structure consists of 21399 atoms under periodic boundary conditions in a high aspect ratio configuration approximately 23 nm in width and 16 nm in height, but only 1 nm (5 atoms) in thickness. Its six grains were created by Voronoi construction around randomly selected locations. All the grains have a common [110] direction lying along the normal to the plane visualized in figure 1 (i.e. the visualized plane is a (110) plane for each grain). Consequently, all the grain boundaries in this model are pure tilt in character: there are no twist boundaries present. Because of this restriction, not all grain boundary orientations that are possible in a bulk columnar granular material are admissible in the

model system studied here. There is no requirement for the grain boundaries to be symmetrical tilt boundaries, however, and in fact most are asymmetrical. The information in table 1 describes each of the grain boundaries identified in figure 1 in its as-constructed state.

The as-constructed quasi-columnar nc-Si structure was annealed for about 15 ns at 950 K, just below the glass transition temperature of SW a-Si [24]. After annealing, the nc-Si structure was quenched down to the target deformation temperature of 300 K. Although some minimal migration of high angle boundaries was observed, no noticeable changes in either the size or orientation of the grains or in the structure of intergranular regions was observed as a result of annealing, indicating that the initial atomic configuration of the investigated model system corresponds to reasonably well-relaxed nc-Si.

The structure of grain boundary atomic environments in the model nc-Si system was characterized by local distributions of distances between atom pairs found in the grain boundaries. The values G(r) of these local radial distribution functions (RDFs) are plotted in figure 2. The grain boundary atoms used in computing these functions were located by the method of Bernstein *et al*. [39] and are visualized in figure 1. While in a-Si no significant ordering is found beyond the second nearest neighbor distance [24], figure 2 shows that the three first nearest neighbor peaks are clearly discernable in the RDFs for the grain boundaries in the model nc-Si system, suggesting a high degree of crystallinity. By contrast, previous studies using the Stillinger-Weber Si potential have indicated that the configuration of atoms found in intergranular regions closely resembles that of a-Si [20, 21]. Those studies, however, have focused on high-energy twist grain boundaries—such as the (100) $\Sigma 29$ twist boundary [20]—and on the relatively more disordered material in grain boundary junctions [21]. The model system studied here contains no twist boundaries and only a small volume fraction of grain junction material due to the columnar morphology. Nevertheless, the RDF found for grain boundaries in the initial undeformed nc-Si is not inconsistent with the presence of solid-like a-Si, whose RDF is very similar to that of crystalline Si [23, 24]. The nearest neighbor bond angle distribution functions of grain boundary material—which showed a single broadened peak centered on the angle of $\cos^{-1}\left(-\frac{1}{3}\right) \approx 109.5^\circ$—also admit the possible presence of solid-like a-Si.

4. Mechanical response

The quasi-columnar nc-Si structure described above was deformed by the method discussed in section 2. Plastic deformation was conducted for three different initial externally applied pressures, i.e. for three different initial system-wide dilatations. Figures 3(a) and 3(b) present the dependencies of deviatoric stress and system pressure on total deviatoric strain. Figure 3(a) demonstrates a high deviatoric yield stress followed by strain softening. The level of this yield stress normalized by the shear modulus of diamond-cubic crystalline SW Si ($\mu = 60.3$ GPa [16]) is about 0.066, a value which compares favorably with that deduced for nanocrystalline nc-TiN/a-Si_3N_4 ceramic composite coatings [40], namely 0.086. Figure 3(a) also shows, however, that after strain softening the deformed nc-Si system exhibits a gradual elevation of flow stress beginning at about $\bar{\varepsilon}(\varepsilon) = 0.34$ total applied deviatoric strain. The cause for this elevation is addressed in section 4.2.

The system pressure response shown in figure 3(b) exhibits two peculiarities: an initial drop in system pressure observed for all three levels of initially applied dilatation as well as a sudden release of negative pressure at about $\bar{\varepsilon}(\varepsilon) = 0.16$ total deviatoric strain in the case of plastic deformation of the nc-Si structure with initially high negative pressure. These two phenomena are explained in sections 4.1 and 4.3, respectively.

4.1 Creation of liquid-like atomic environments

Figure 2 shows a typical local RDF for grain boundary material after plastic deformation to large strain. Like the one obtained for the initial undeformed configuration, this RDF exhibits three distinct nearest neighbor peaks, suggesting significant crystallinity in the intergranular regions. Unlike in the undeformed case, however, the grain boundary RDF in the deformed system contains the telltale sign of the presence of liquid-like a-Si, namely a hump between the first and second nearest neighbor peaks [23, 24].

Applying the distinction between liquid-like and solid-like atomic environments described in section 2 and developed in reference 24, the evolution of the mass fraction of liquid-like environments ϕ

during deformation can be found for all three initial pressures of the investigated quasi-columnar nc-Si structure. Figure 3(c) plots the evolution of ϕ as a function of total applied deviatoric strain for the nc-Si system deformed at three different initial dilatations. The system contains low but finite initial values of ϕ, demonstrating that some liquid-like a-Si is present in the grain boundaries even prior to any deformation. During plastic deformation, ϕ rises markedly for all three initial dilatations of the nc-Si system. Since liquid-like a-Si atomic environments are more dense than both solid-like a-Si or crystalline Si ones, the increasing values of ϕ demonstrated in figure 3(c) explain the pressure decreases observed in all three system pressure versus total deviatoric strain curves shown in figure 3(b). The largest rises in the values of ϕ occur in regimes of total externally applied strain corresponding to strain softening in figure 3(a). This observation implies that liquid-like atomic environments serve as plasticity carriers in intergranular regions of nc-Si, much as they do in bulk a-Si [23, 24].

Figure 4 visualizes the location of liquid-like atomic environments in a system past the strain-softening stage of its flow behaviour, indicating that most such environments are aligned within a single system-spanning zone of intergranular material. This zone is rather narrow, with a typical thickness of about 2 or 3 atomic diameters. Annealing of a nc-Si system with such a distribution of liquid-like atomic environments at 950 K for about 4 ns removes the entire excess liquid-like mass fraction accumulated as a result of plastic deformation. This finding confirms that this easily flowing type of a-Si is metastable. Due to time scale constraints, however, the rate of annealing-out of liquid-like atomic environments at room temperatures is currently inaccessible to MD simulation.

The local RDFs of grain boundary regions in the nc-Si configuration after deformation and after post-deformation annealing are shown in figure 2. The absence of a hump below the second nearest neighbor peak in the latter confirms the removal of most of the liquid-like a-Si during annealing. Comparison of this RDF with that of intergranular regions before deformation indicates that the states of grain boundary material prior to deformation and after post-deformation annealing are indistinguishable.

4.2 Plasticity in zones of easy flow

The method of distinguishing between linear elastically deforming matrix and inelastically transforming inclusion introduced in section 2 and developed in reference 25 can be applied to consecutive configurations of the quasi-columnar nc-Si system undergoing plastic flow. In this way, portions of the nc-Si system currently undergoing inelastic transformation as well as those that have transformed at some previous time during the course of deformation can be distinguished from those that have only undergone linear elastic flexing. Figure 5 shows visualizations of these three types of atomic environments at three stages of deformation of the quasi-columnar nc-Si structure with initial pressure of $p(\tau) = 0.05$ GPa.

As shown in figure 5(a), at a total deviatoric strain of $\bar{\varepsilon}(\varepsilon) \approx 0.08$ inelastic transformations have occurred primarily in a series of mutually parallel or perpendicular intergranular regions such as the ones enclosed in the ellipses. These transformations have allowed neighboring grains to accommodate the formation of the incipient zone of easy plastic flow visualized previously in figure 4 in terms of its concentration of liquid-like atomic environments. In figure 5(b) this zone (indicated by solid lines) has become fully developed and spans the entire system. Note that the thickness of the zone as defined by the material that has undergone inelastic transformation at some time during the deformation process is about 5 to 7 atomic diameters or about twice as wide as the liquid-like a-Si zone visualized in figure 4. This observation indicates that during the course of plastic flow, local inelastic transformations in intergranular regions are aided by cooperative deformation at the edges of neighboring crystallites, but that in the long term this cooperative deformation does not result in the destruction of crystalline order in the regions where it has occurred.

Finally, figure 5(c) visualizes the quasi-columnar nc-Si system at such a high level of deformation that the previously formed zone of easy flow (denoted by dashed lines) has rotated out of the plane of maximum resolved shear stress. Inelastic transformations at this stage of deformation have begun to localize into new zones of easy flow (solid lines) that are better aligned with the maximum resolved shear stress direction. New liquid-like a-Si atomic environments are formed in these incipient flow zones, leading to the increase of ϕ observed above $\bar{\varepsilon}(\varepsilon) \approx 0.40$ in figure 3(c). The emergence of these new flow zones

suggests an explanation for the rise in flow resistance observed in the composite response of the nc-Si system plotted in figure 3(a). Namely, this rise can be traced back to the high initial yield stress associated with the formation of new liquid-like a-Si material during the emergence of new zones of easy flow after the previously active flow zone had rotated out of a plane of maximum resolved shear stress.

To confirm the above hypothesis, the mean resolved shear stress on the initially formed zone of easy flow (visualized in figure 5(b)) was calculated and plotted in figure 6(a). Unlike the dependence of overall system deviatoric stress on total strain, this mean resolved shear stress shows no tendency to increase, indicating that the rise in overall system deviatoric stress is due to the flow geometry and not to changes in the material's intrinsic mechanical properties. The total shear displacement along the flow zone was also calculated and is shown in figure 6(b). During steady state flow along the zone, this displacement increases at an approximately constant rate. As the initially formed zone of easy flow rotates out of the plane of maximum resolved shear stress, however, the rate of shear displacement along the flow zone attenuates. Shear displacement along the zone eventually ceases once plastic deformation along the newly formed zones shown in figure 5(c) becomes easier than along the initially formed zone.

In addition to localization of plasticity along zones of easy flow, deformation of the model nc-Si system to large strain is accompanied by several processes that accommodate microstructural compatibility. One example of such a process is grain rotation. The rotation of the grain marked 'C' in figure 5(b) has been plotted in figure 6(b) as a function of total system deviatoric strain. The initial jerky rotation of the grain takes place during the first stages of the emergence of the initial zone of easy flow. Once steady state flow along the zone has developed, the grain rotates at a constant rate. The rate of rotation of the grain decreases when plasticity along the initially formed zone of easy flow attenuates.

Another example of a process that accommodates microstructural compatibility during plastic flow is the deformation-induced creation of new crystal grains, as previously observed by Yamakov *et al.* [7]. Several new crystal grains that have emerged during plastic flow of the nc-Si structure studied here are marked by roman numerals in figure 5(c).

4.3 Release of high negative pressure

Identification of liquid-like a-Si atomic environments yields insight into the cause of the sudden release of negative pressure during plastic deformation at an initial (negative) pressure of $p(\tau) = -0.96$ GPa, as seen in figure 3(b). Figure 7 shows the configuration of the system at the moment of pressure release. It can immediately be seen that a microvoid nucleates at the point in the zone of plastic flow (dashed lines) indicated by the circle. During the course of later deformation this void elongates into a microcrack along the zone of easy flow. Since the simulation is conducted under constant volume, however, this microcrack does not propagate and closes upon further deformation.

The mean tensile stress across the plane of easy flow at the nucleation site of the microvoid was determined for the entire course of deformation and is plotted in figure 8. The release of system negative pressure and nucleation of the microvoid both occur when the mean tensile stress across the microvoid nucleation site in the zone of easy flow reaches a maximum. The reason for the nucleation of the microvoid within the zone of easy flow can be understood in terms of the properties of liquid-like atomic environments. Since these atomic environments are denser than the crystalline Si and solid-like a-Si ones, their creation during the course of plastic flow is unable to relieve the buildup of negative pressure. Indeed, as discussed in section 4.1, it exacerbates that buildup. Therefore, relief of the mounting tensile stress requires a mechanism not involving plastic flow. Since no mechanism that could relieve the tensile stress while simultaneously preserving microstructural compatibility was available for the particular atomic configuration shown in figure 7, the tensile stress had to be relieved through a mechanism that does not preserve microstructural compatibility, such as the observed microvoid nucleation.

5. Discussion

The picture of plasticity in nc-Si revealed by the simulations described above can be summarized as follows. Plastic deformation occurs entirely in intergranular material: no dislocation-mediated plasticity was observed inside the crystalline grain interiors. Grain rotation and refinement allows deforming

intergranular regions to align into well-defined system-spanning zones of easy flow. So long as microstructural compatibility can be accommodated, plastic flow remains entirely confined to these zones. If, however, there should emerge a stress concentration that cannot be relaxed by any mechanism that simultaneously preserves microstructural compatibility, nano-scale voids or cracks may be formed in the zones of easy flow. If plastic flow proceeds to strains so large that the initially formed zones of easy flow have rotated significantly out of the planes of maximum resolved shear stress, new zones of easy flow may form by the same processes by which the initial ones were created. At fully developed plasticity the active plastic shear zones set up a rectangular pattern resembling the slip lines of non-hardening plasticity in the mathematical theory of plasticity [41]. Such restructuring of grains into a set of squares separated by freely sliding grain boundaries to reduce the overall plastic resistance has been widely observed, particularly in cyclic deformation at elevated temperatures [42].

Plastic flow to large strain in nc-Si involves several mechanisms working in concert. These can be broadly grouped into three categories:

1. Plastic deformation of intergranular material with grain interiors undergoing only elastic flexure;
2. Mechanisms of microstructural compatibility accommodation;
3. Nucleation of nano-scale voids or cracks when compatibility demands it.

The first of these three groups can be treated by analogy to plastic deformation in pure a-Si. As shown in previous studies [23-26], well-relaxed a-Si contains a low mass fraction of liquid-like atomic environments, ϕ; most environments may be described as solid-like a-Si. During the early stages of plastic flow in a-Si, solid-like environments are converted to denser, more easily flowing liquid-like ones. Consequently, the increase in ϕ is accompanied by strain softening and deformation-induced volume contraction. During fully-developed steady state flow in pure a-Si, the average number of solid-like atomic environments that are converted into liquid-like ones equals the number that undergo the reverse process, resulting in a ϕ value that is constant on the time-average. As would be expected, the plastic shear resistance and volume of a-Si in this state is also constant on the time-average. If the external load is removed from an a-Si system undergoing steady-state flow, its ϕ value does not change. If annealed just below the glass transition of a-Si, however, ϕ decreases within a few nanoseconds to the value characteristic of well-annealed a-Si.

All the processes described above have their analogues in grain boundary plasticity in nc-Si. Although exhibiting a high degree of crystallinity, intergranular material in well-relaxed nc-Si may also be described as solid-like a-Si. The onset of plasticity in this material is accompanied by the creation of denser, easily flowing liquid-like a-Si atomic environments. Strain softening and a rise in negative pressure at constant total volume (equivalent to volume contraction at constant total pressure) are simultaneously observed. In a given flow zone, ϕ is constant on the time-average once steady-state plastic flow has developed in that zone. As in the case of pure a-Si, this steady state in the easy-flow shear zones is a result of the average number of solid-like atomic environments converted into liquid-like ones being equal to the average number undergoing the reverse process. At large plastic strains when active shear zones rotate away from planes of maximum resolved stress, the high liquid-like a-Si concentration in such zones remains dormant and enriches the overall liquid-like material concentration in the polycrystal. As in pure a-Si, however, if an nc-Si structure that has been deformed to large strain is subsequently annealed just below the glass transition temperature of a-Si, ϕ is reduced to pre-deformation levels within four nanoseconds.

Due to their analogous plastic deformation behaviours, intergranular material in nc-Si may be modeled constitutively as a-Si, with the proviso that all additional required sequential local shear transformations must develop in the narrow confines of the active shear zones. There remain, however, at least two questions that must be clarified before a full understanding of grain boundary plasticity in nc-Si is obtained. The first concerns the role of thermal annealing in reducing the mass fraction of liquid-like material ϕ present during fully developed flow. As discussed earlier, high temperature annealing of a structure that has a large ϕ value quickly reduces that value to its equilibrium level. While the rates of annealing out of liquid-like a-Si that can be determined through high temperature annealing simulations are far faster than the ones that would be encountered in low temperature plastic deformation, a significant reduction in the amount of liquid-like a-Si present during plastic flow may nevertheless also be expected due to lower temperature annealing over longer time spans than those currently accessible through MD

simulations. Such an eventuality may well be important in settings of technological interest, which are likely to involve much lower deformation strain rates than the rates used in the simulations presented here. A reduction in ϕ during steady state flow due to annealing would then result in a lower volume contraction and higher flow stress than would have been expected on the basis of high strain rate studies.

The other unanswered question relevant to constitutive modeling of intergranular material in nc-Si involves accounting for the immediate proximity of crystalline material. As pointed out in section 4.2, the regions of crystalline grains that are adjacent to flowing intergranular material also undergo some inelastic deformation, although in the long run this deformation does not destroy crystalline order in those regions. This unusual behaviour suggests that 'grain edge' material may exhibit properties that are transitional between those of the neighboring amorphous flowing intergranular material on the one hand and those of the crystalline non-deforming material on the other. Such transitional properties may mirror the structural indeterminacy of grain boundary material discussed in section 3. The nature of plasticity in 'grain edges', its influence on the flow properties of intergranular material, and its role in the overall process of plastic deformation in nc-Si has yet to be fully investigated. Such an investigation must attend to the effects of confinement of the elemental shear processes of plasticity in a-Si into the narrow active shear zones seen in nc-Si.

The second set of mechanisms relevant to plasticity in nc-Si contains those that accommodate microstructural compatibility. Two such mechanisms have been observed in the simulations presented here, namely grain rotation and deformation-induced creation of new grains. The latter has already been observed by Yamakov *et al.* [7], who have attempted to interpret the creation of grains in terms of crystal plasticity processes. Nonetheless, a more extensive study dedicated to such mechanisms is in order, both because they are relatively poorly understood and because of their crucial importance to the third set of deformation mechanisms: formation of nano-scale voids and cracks. As shown in section 4.3, nucleation of nano-voids and cracks occurs if the magnitude of a local stress concentration reaches values approaching the theoretical strength of decohesion. Nevertheless, the emergence of such intense stress concentrations is only possible if there exist no microstructural compatibility-accommodation mechanisms that would be able to relax these stress concentrations without having to form voids or cracks. A better understanding of the possible mechanisms of microstructural accommodation therefore increases our ability to predict what situations may lead to nucleation of voids and cracks.

Conclusion

Plasticity in a model quasi-columnar nanocrystalline silicon (nc-Si) system has been investigated using molecular dynamics simulations at T=300 K. It was shown that plastic flow takes place exclusively in intergranular regions that contain material that can be characterized as liquid-like amorphous silicon (a-Si). During fully developed plasticity, inelastic deformation is confined to intergranular zones of easy flow that span the entire system and make up a pattern resembling the slip lines of the mathematical theory of plasticity. As an active flow zone rotates out of the plane of maximum resolved shear stress during deformation to large strain, new zones of easy flow are formed.

During plastic flow, microstructural compatibility is accommodated by processes such as rotation of existing grains as well as deformation-induced creation of new grains. Nevertheless, certain stress concentrations that cannot be relaxed by any available mechanism that also preserves microstructural compatibility may also emerge during plastic flow. Such stress concentrations can serve as nuclei for the formation of nano-scale voids or cracks.

Acknowledgements

We would like to thank D. Wolf, P. Keblinski, and V. Yamakov for making their MD codes available to us. We are also grateful to S. Veprek, M. Bazant, S. Yip, C. Ashe, and D. Danielson for useful discussions. The atomic structure visualizations presented here were generated using the AtomEye program [43]. This manuscript is based upon work supported by the NSF Graduate Fellowship, the Los Alamos National Laboratory Director's Postdoctoral Fellowship, and the Defense University Research Initiative on NanoTechnology (DURINT) on 'Damage- and Failure-Resistant Nanostructured and Interfacial Materials',

funded at the Massachusetts Institute of Technology by the Office of Naval Research under grant N00014-01-1-0808.

References

[1] E. O. Hall, Proc. Phys. Soc. Sect. B **64** 747 (1951).
[2] N. J. Petch, Journal of the Iron and Steel Institute **174** 25 (1953).
[3] M. F. Ashby, Phil. Mag. **21** 399 (1970).
[4] J. Schiotz and K. W. Jacobsen, Science **301** 1357 (2003).
[5] S. Yip, Nature 391 **532** (1998).
[6] J. Schiotz, F. D. Di Tolla, and K. W. Jacobsen, Nature **391** 561 (1998).
[7] V. Yamakov, D. Wolf, S. R. Phillpot, A. K. Mukherjee, and H. Gleiter, Nature Materials **1** 45 (2002).
[8] H. Van Swygenhoven, P. M. Derlet, and A. G. Froseth, Nature Materials **3** 399 (2004).
[9] A. S. Argon and S. Yip, Accepted for publication in Phil. Mag. (2006)
[10] Q. Ren, B. Joos, and M. S. Duesbery, Phys. Rev. B **52** 13223 (1995).
[11] T. D. Shen, C. C. Koch, T. L. McCormick, R. J. Nemanich, J. Y. Huang, and J. G. Huang, J. Mat. Res. **10** 139 (1995).
[12] S. Veprek, J. Vac. Sci. Technol. A **17** 2401 (1999).
[13] H. Kahn, L. Chen, R. Ballarini, and A. H. Heuer, Acta Mater. **54** 667 (2006).
[14] F. H. Stillinger and T. A. Weber, Phys. Rev. B **31** 5262 (1985).
[15] J. Tersoff, Phys. Rev. Lett. **56** 632 (1986).
[16] H. Balamane, T. Halicioglu, and W. A. Tiller, Phys. Rev. B **46** 2250 (1992).
[17] M. Z. Bazant, E. Kaxiras, and J. F. Justo, Phys. Rev. B **56** 8542 (1997).
[18] M. D. Kluge and J. R. Ray, Phys. Rev. B **37** 4132 (1988).
[19] W. D. Luedtke and U. Landman, Phys. Rev. B **40** 1164 (1989).
[20] P. Keblinski, S. R. Phillpot, D. Wolf, and H. Gleiter, Phys. Rev. Lett. **77** 2965 (1996).
[21] P. Keblinski, S. R. Phillpot, D. Wolf, and H. Gleiter, Acta Mater. **45** 987 (1997).
[22] S. Sastry and C. A. Angell, Nature Materials **2** 739 (2003).
[23] M. J. Demkowicz and A. S. Argon, Phys. Rev. Lett. **93** 025505 (2004).
[24] M. J. Demkowicz and A. S. Argon, Phys. Rev. B **72** 245205 (2005).
[25] M. J. Demkowicz and A. S. Argon, Phys. Rev. B **72** 245206 (2005).
[26] A. S. Argon and M. J. Demkowicz, Phil. Mag. **86** 4153 (2006).
[27] J. Q. Broughton and X. P. Li, Phys. Rev. B **35** 9120 (1987).
[28] A. S. Argon, in *Physical Metallurgy*, edited by R. W. Cahn and P. Haasen (North-Holland, Amsterdam, 1996), chapter 21.
[29] F. A. McClintock and A. S. Argon, *Mechanical Behavior of Materials* (Addison-Wesley, Reading, MA, 1966).
[30] D. Brown and S. Neyertz, Mol. Phys. **84** 577 (1995).
[31] K. Maeda and S. Takeuchi, J. Phys. F **12** 2767 (1982).
[32] V. M. Glazov, S. N. Chizhevskaia, and N. N. Glagoleva, *Liquid Semiconductors* (Plenum Press, New York, 1969), chapter 3.
[33] A. S. Argon and L. T. Shi, in *Amorphous Materials: Modeling of Structure and Properties*, edited by V. Vitek (Metallurgical Society of AIME, Warrendale, Pa, 1983), page 279.
[34] D. Deng, A. S. Argon, and S. Yip, Philos. Trans. Roy. Soc. Lond. Ser. A **329** 549 (1989).
[35] D. Deng, A. S. Argon, and S. Yip, Philos. Trans. Roy. Soc. Lond. Ser. A **329** 575 (1989).
[36] D. Deng, A. S. Argon, and S. Yip, Philos. Trans. Roy. Soc. Lond. Ser. A **329** 595 (1989).
[37] D. Deng, A. S. Argon, and S. Yip, Philos. Trans. Roy. Soc. Lond. Ser. A **329** 613 (1989).
[38] J. D. Eshelby, Proc. Roy. Soc. Lond. Ser. A **241** 376 (1957).
[39] N. Bernstein, M. J. Aziz, and E. Kaxiras, Phys. Rev. B **61** 6696 (2000).
[40] A. S. Argon, M. J. Demkowicz, and S. Veprek, AIP Conf. Proc. **712** 3 (2004).
[41] R. Hill, *The Mathematical Theory of Plasticity* (Clarendon Press, Oxford, 1950).
[42] M. Kitagawa, in ASTM-STP 519 (1973), page 58.
[43] J. Li, Mod. Simul. Mater. Sci. Eng. **11** 173 (2003).

Tables

Table 1: For the as-constructed configuration of each of the grain boundaries labeled in figure 1, this table gives the pair of neighboring grains, misorientation angle, a possible coincident site lattice (CSL) Σ number, and the deviation from the exact CSL misorientation angle.

Grain boundary	Neighboring grain 1	Neighboring grain 2	Misorientation angle (deg)	CSL Σ	Deviation from CLS (deg)
1	A	E	23.43	19a	3.1
2	A	B	124.68	41c	0.56
3	B	C	101	N/A	N/A
4	C	D	67.13	3	3.4
5	A	D	90.81	17b	2.56
6	B	E	101.25	N/A	N/A
7	B	C	101	N/A	N/A
8	C	D	67.13	3	3.4
9	D	E	67.38	3	3.15
10	A	E	23.43	19a	3.1
11	E	F	76.32	3	5.79
12	B	E	101.25	N/A	N/A
13	C	E	0.25	1	0.25
14	C	D	67.13	3	3.4
15	D	E	67.38	3	3.15
16	D	F	8.94	1	8.94
17	E	F	76.32	3	5.79
18	B	F	24.93	19a	1.6
19	A	B	124.68	41c	0.56
20	B	C	101	N/A	N/A
21	A	D	90.81	17b	2.56
22	A	F	99.75	N/A	N/A

Figure captions

Figure 1: Visualization of the quasi-columnar nc-Si structure whose plastic deformation behaviour was investigated in this study. The structure consists of 21399 atoms under periodic boundary conditions in a configuration approximately 23 nm in width and 16 nm in height, but only 1 nm (5 atoms) in thickness. Light atoms correspond to diamond cubic crystalline Si while dark ones represent grain boundaries. Grain boundary atoms were found by the method of Bernstein *et al.* [39]. Numbers denote grain boundaries while letters denote grains. Details of structure for the as-constructed grain boundaries labeled here are provided in table 1.

Figure 2: Values G(r) of local radial distribution functions (RDFs) evaluated for grain boundary material in its initial undeformed state (circles), after deformation to 117% total deviatoric strain (squares), and after post-deformation annealing at 950K for 4ns (triangles). Plots have been offset by increments of four for clarity. The dashed lines indicate the position of peaks in the RDF for perfect diamond cubic Si at zero pressure. The first three nearest neighbor peaks are distinctly discernable in all three grain boundary states, indicating a high degree of crystallinity in each. The RDF for intergranular material after deformation exhibits a hump between the first and second nearest neighbor peaks (indicated by the arrow) that is characteristic of liquid-like a-Si [23, 24]. Annealing of the deformed configuration, however, removes the liquid-like a-Si signature generated during plastic flow.

Figure 3: The dependence of (a) deviatoric stress $\overline{\sigma}(\tau)$, (b) system pressure $p(\tau)$, and (c) liquid-like mass fraction ϕ on the total deviatoric strain $\overline{\varepsilon}(\varepsilon)$ during constant-volume plane strain plastic deformation of the model nc-Si system at a temperature of 300K. Deformation was carried out for the nc-Si system at three different initial dilatations, corresponding to different values of initial externally applied pressure. The curves in (a) have been offset by increments of 1GPa for clarity. Similarly, the curves in (c) have been offset by increments of 0.02.

Figure 4: Visualization of the distribution of liquid-like atomic environments in the quasi-columnar nc-Si system initially at a pressure of $p(\tau) = 0.05$ GPa when plastically deformed to $\overline{\varepsilon}(\varepsilon) \approx 0.25$ total deviatoric strain. Dark atoms are liquid-like a-Si. The solid lines indicate the zone where most of the intergranular liquid-like a-Si has been created.

Figure 5: Visualization of the nc-Si structure with initial pressure of $p(\tau) = 0.05$ GPa at stages of plastic deformation corresponding to total deviatoric strains of (a) $\overline{\varepsilon}(\varepsilon) \approx 0.08$, (b) $\overline{\varepsilon}(\varepsilon) \approx 0.25$, and (c) $\overline{\varepsilon}(\varepsilon) \approx 0.53$. The darkest atoms denote environments currently undergoing inelastic transformation, those with medium darkness indicate ones that have transformed inelastically at some prior time during the course of deformation, and the lightest ones represent those environments that have only undergone elastic flexing and have not experienced inelastic transformation. The ellipses in (a) show intergranular regions where plastic deformation initially localizes. The solid lines in (b) denote a zone of fully developed plastic flow. The rotation of the grain marked 'C' during the course of plastic deformation is plotted in figure 6(b). In (c), the dashed lines indicate the same zone of plastic flow as the one shown in (b) while the solid lines denote emergent new zones of plastic flow whose orientation is better aligned with the direction of maximum resolved shear stress. The roman numerals indicate new grains that have been created during the course of plastic deformation.

Figure 6: (a) The total system deviatoric stress exhibits a tendency to increase once a total deviatoric strain of about $\overline{\varepsilon}(\varepsilon) = 0.34$ (solid vertical line) has been reached. Nonetheless, the mean resolved shear stress on the initially formed zone of easy plastic flow shown in figure 5(b) does not show the same tendency, demonstrating that the rise in system deviatoric stress above $\overline{\varepsilon}(\varepsilon) = 0.34$ is not due to a change in the intrinsic mechanical properties of intergranular material. (b) As the initially formed zone of easy plastic flow progressively rotates out of the plane of maximum resolved shear stress, flow along this zone also attenuates as evidenced by the decreasing rate of shear displacement along the zone. As plasticity on the

easy flow zone attenuates, so do the processes that accommodate microstructural compatibility, such as rotation of the grain the marked 'C' in figure 5(b).

Figure 7: Visualization of the quasi-columnar nc-Si structure initially at a (negative) pressure of $p(\tau) = -0.96$ GPa at a stage of plastic deformation corresponding to a total strain of $\bar{\varepsilon}(\varepsilon) \approx 0.16$. Dark-coloured atoms denote liquid-like a-Si environments, as in figure 4. Dashed lines indicate a zone of fully developed easy flow such as the one visualized in figure 5. A microvoid has nucleated in the circled region.

Figure 8: (a) Release of system negative pressure during the course of plastic deformation of the quasi-columnar nc-Si structure initially at a (negative) pressure of $p(\tau) = -0.96$ GPa occurred at about $\bar{\varepsilon}(\varepsilon) = 0.15$ (solid vertical line). Simultaneously (b), the mean tensile stress across the circled region in the zone of easy flow visualized in figure 7 reached a maximum. The release of negative pressure was achieved by the nucleation of a microvoid in that region.

Figures

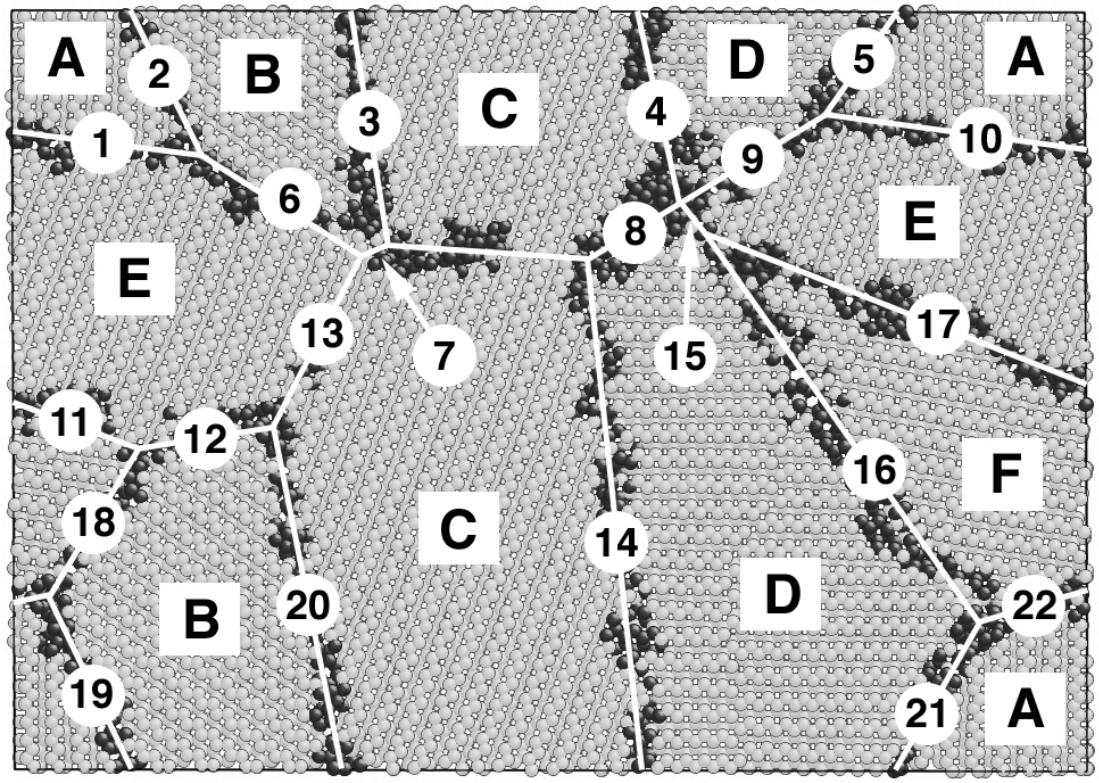

Figure 1

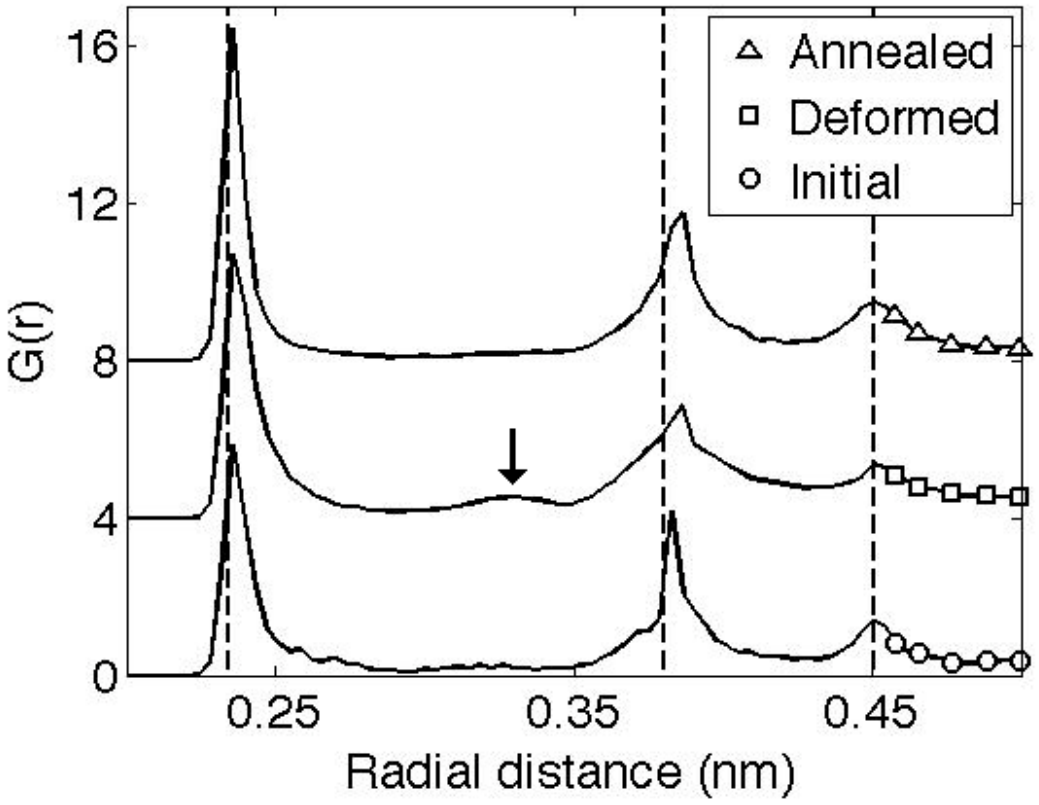
Annealed
Deformed
Initial
16
12
8
4
0
G(r)
0.25
0.35
0.45
Radial distance (nm)

Figure 2

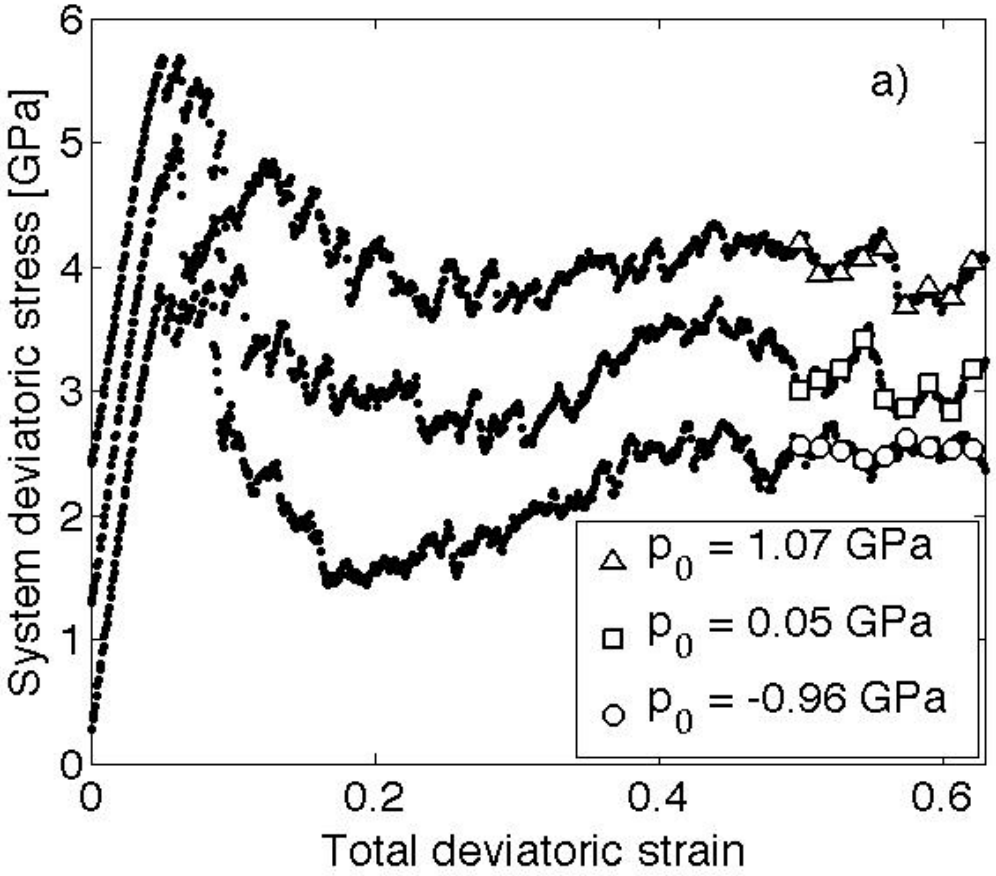
a)
System deviatoric stress [GPa]
Total deviatoric strain
0
1
2
3
4
5
6
0
0.2
0.4
0.6
p_0 = 1.07 GPa
p_0 = 0.05 GPa
p_0 = -0.96 GPa

Figure 3.a)

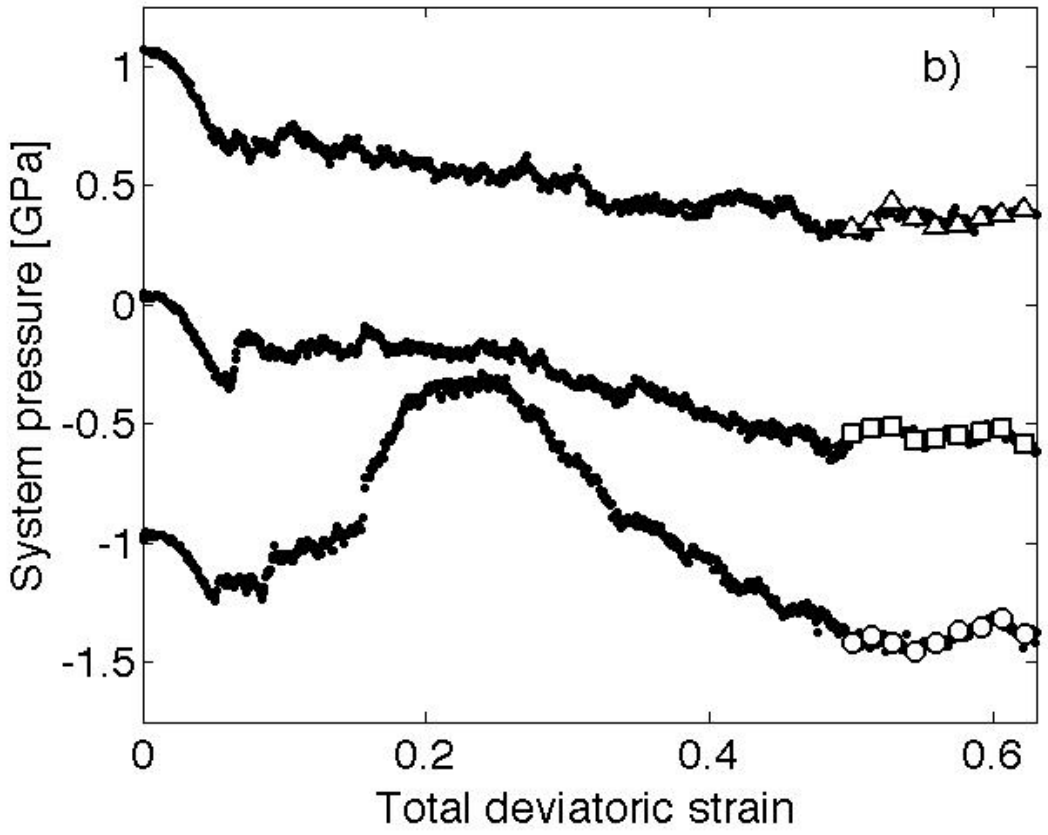
b)
System pressure [GPa]
1
0.5
0
-0.5
-1
-1.5
0
0.2
0.4
0.6
Total deviatoric strain

Figure 3.b)

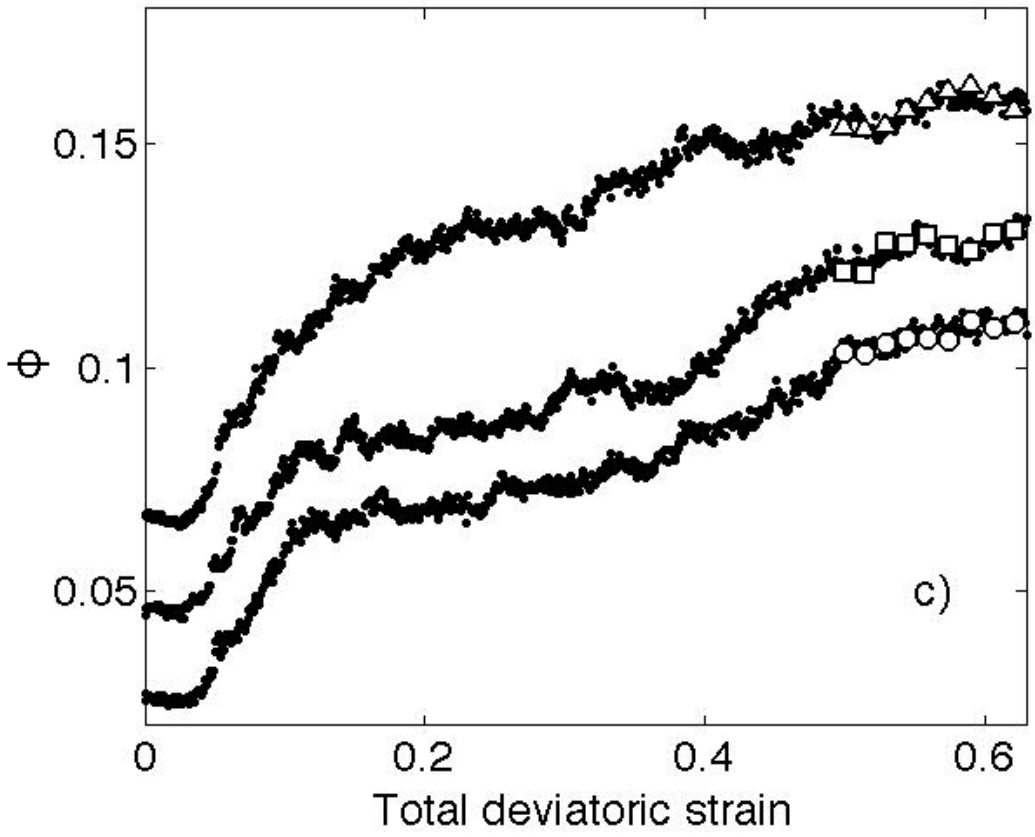

Figure 3.c)

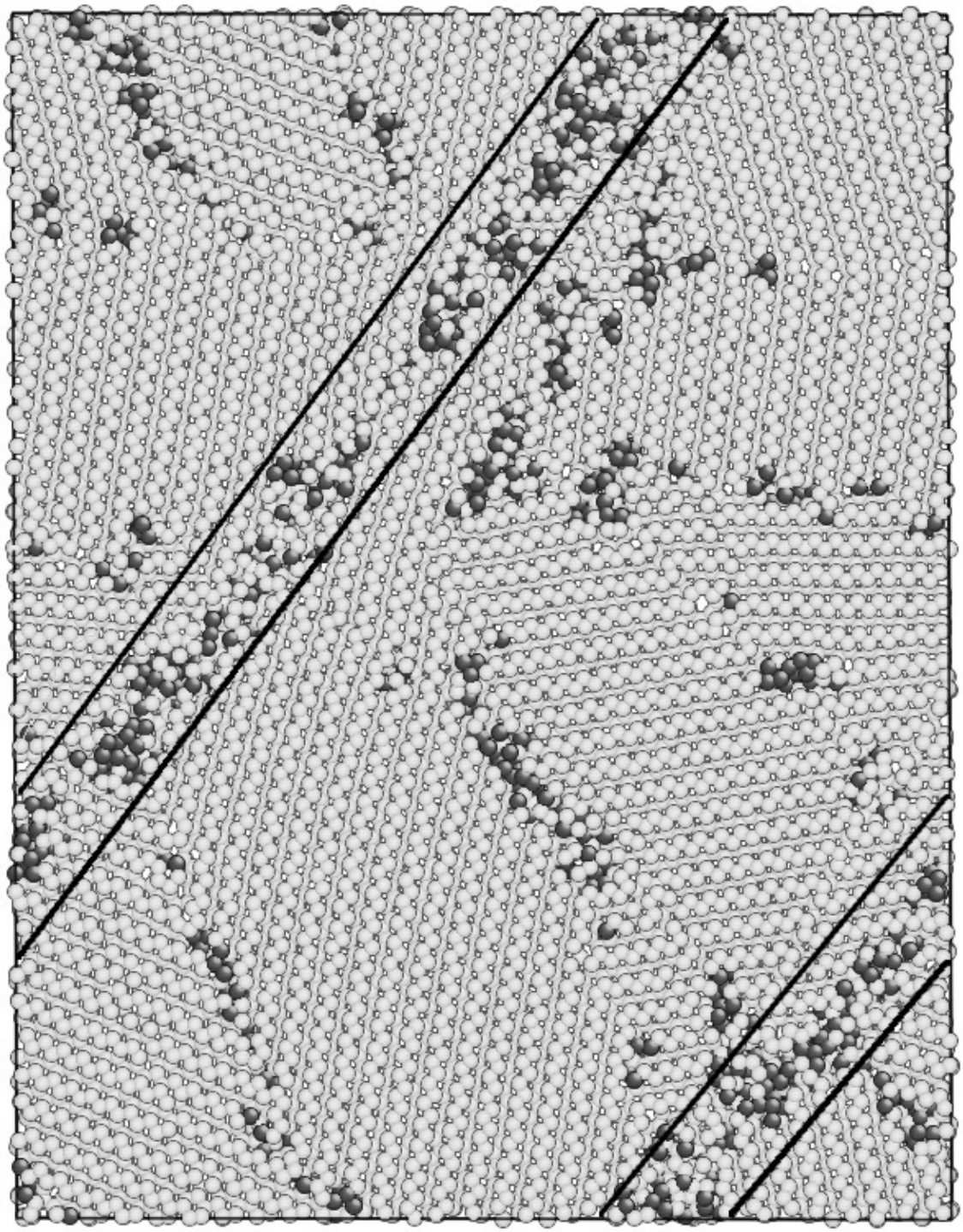

Figure 4

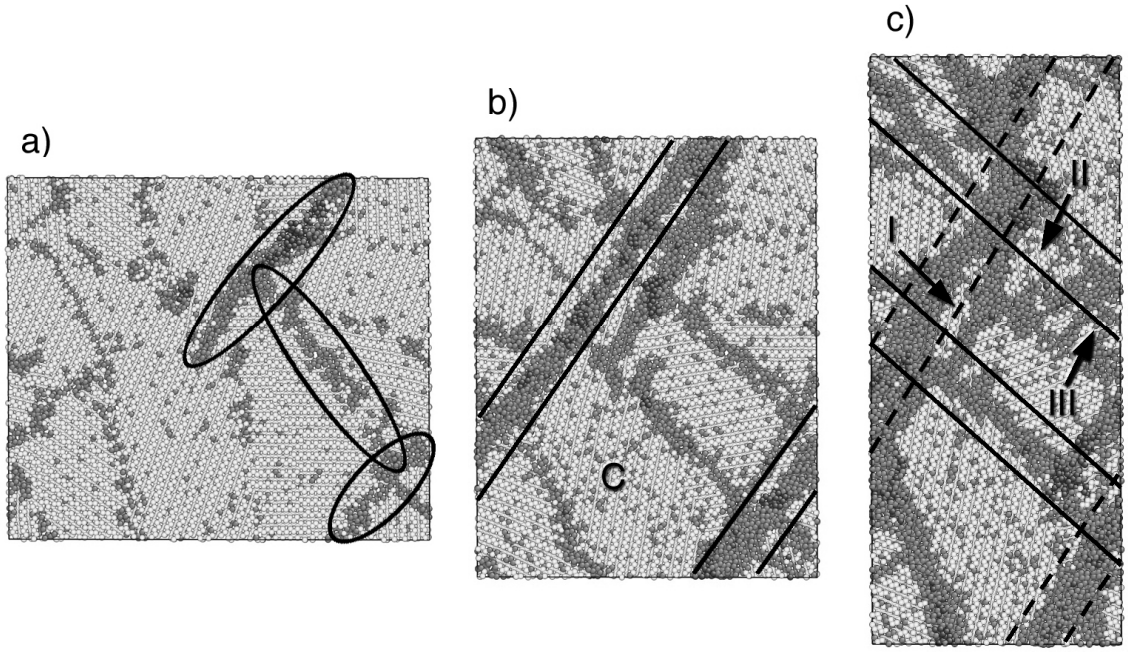

Figure 5

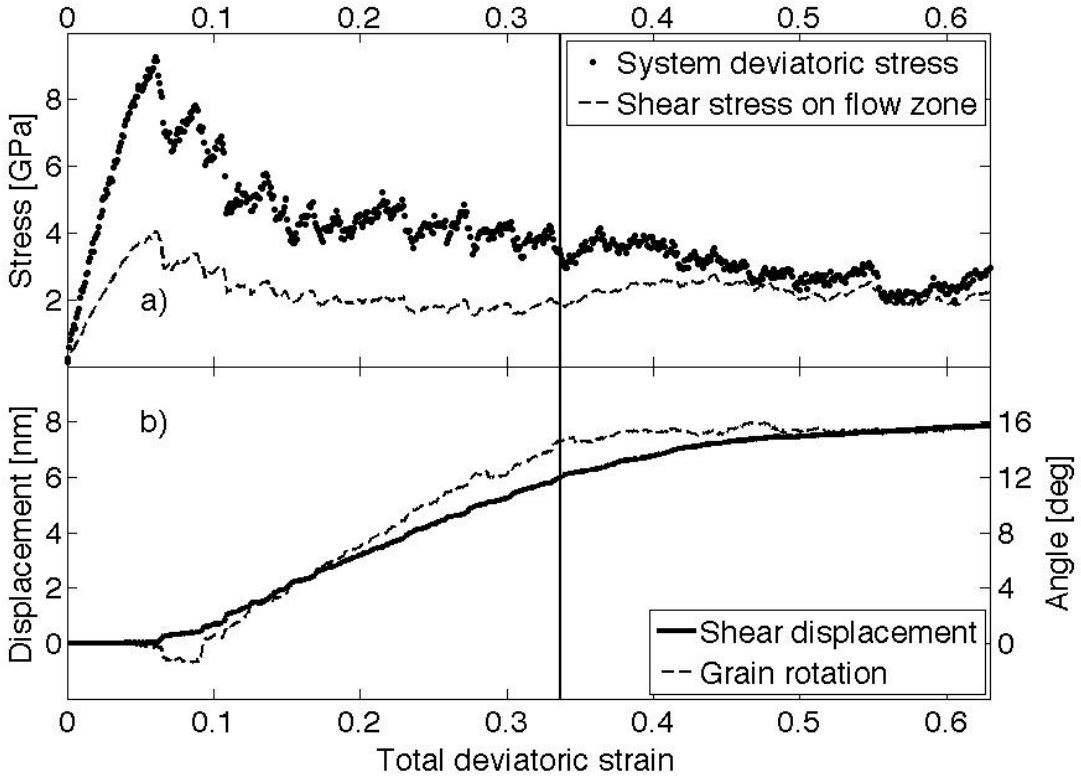

Figure 6

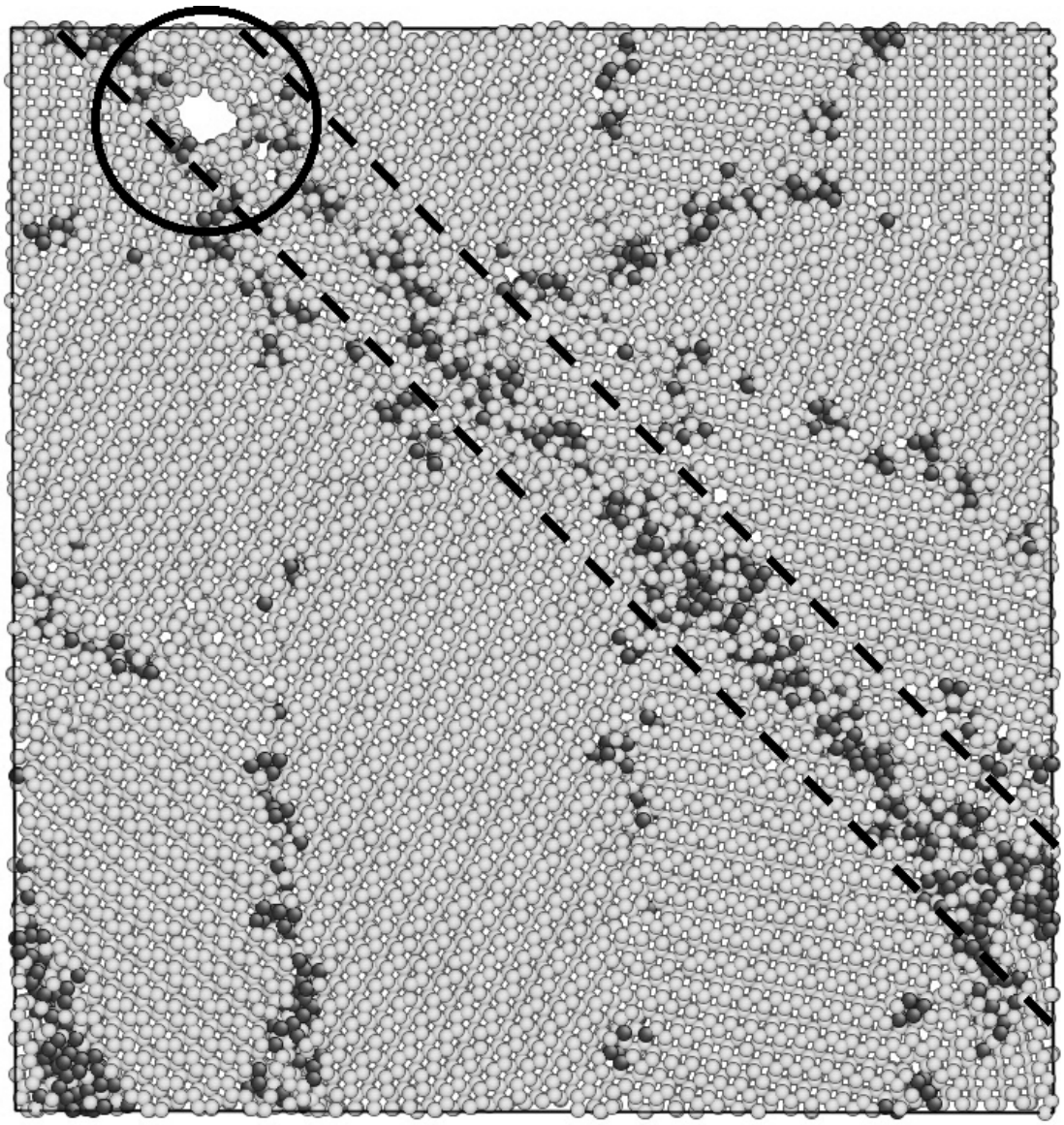

Figure 7

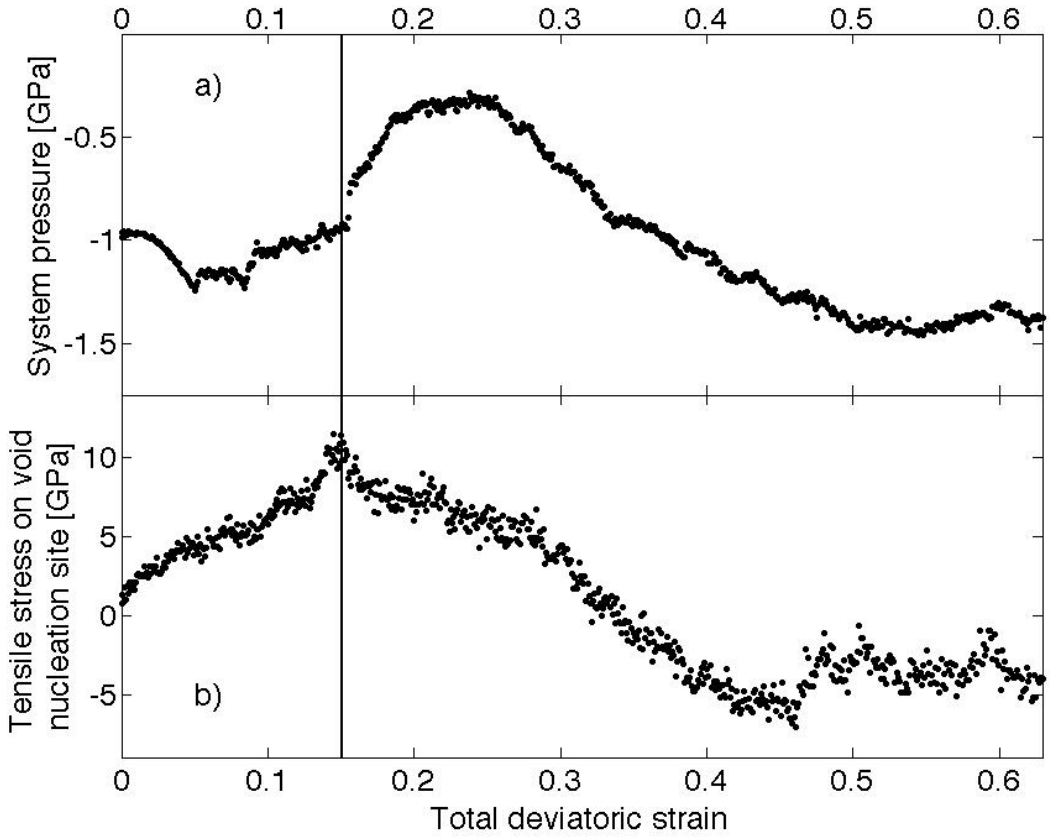
a)
b)
System pressure [GPa]
Tensile stress on void nucleation site [GPa]
Total deviatoric strain
0
0.1
0.2
0.3
0.4
0.5
0.6
-0.5
-1
-1.5
10
5
0
-5

Figure 8